Modeling of the Partial Discharge Process Between the Winding and the Stator of Low Voltage Machines for Traction Applications

Florian Pauli, Moritz Kilper, Niklas Driendl, and Kay Hameyer, *Senior Member, IEEE*

***Abstract*—The application of wide-band-gap-semiconductors in the power-electric circuit of future traction drives leads to an increased stress on the insulation system. This can cause partial discharge, which leads to a rapid breakdown of the insulation and must, therefore, be avoided. To enhance the durability of the insulation system and to fill up the air gaps between the enameled wires, impregnation material is applied. This leads to an increased partial discharge inception voltage between neighboring conductors as the discharge process only occurs in the remaining air enclosures. Due to the change of the electric field distribution, which is caused by the impregnation material, also the threshold voltage for partial discharge between the stator and the winding changes. While so-called twisted pairs are commonly applied to study the partial discharge behavior of the inter-turn insulation isolated from other effects, in this article a specimen that considers the phase-to-ground insulation is proposed.**

***Index Terms*—Electrical machines, insulation system, partial discharge, traction drives.**

I. Introduction

IN ORDER to decrease the losses in the power electronics, a possibility is to change the semiconductor from Silicon Insulated-Gate Bipolar Transistor (Si-IGBT) to Silicon Carbid Metal-Oxide-Semiconductor Field-Effect Transistor (SiC-MOSFET) [1]. Additionally, SiC-semiconductors allow for higher switching frequencies and are therefore particularly suitable for high speed drives. The benefit of the decreased losses is mainly caused by a shorter switching time. It is well known that a faster switching leads to a transient overvoltage in the winding of the electrical motor [2]–[5]. Therefore, the use of wide band gap MOSFETs in modern power electronics for low voltage traction drives causes challenges for the insulation system. Due to the fast switching operation of the semiconductors, transient voltage overshoot effects in the winding system of an electrical machine occur. In combination with an increased voltage level, this overshoot leads to higher electrical stress within the insulation system. Based on the requirements for conventional winding insulation systems, the emerging electrical field can generate partial discharges (PD). In the insulation system of low voltage traction drives PD can occur at several locations: In Fig. 1, the cross section of an exemplary slot is displayed along with the most common locations where PD occurs. The different components of the insulation system can be distinguished into:

- inter-turn insulation: typically made of enameled wire which insulates two adjacent turns from each other
- phase-to-phase insulation: typically made of insulation papers or laminates which insulate two phases from each other
- phase-to-ground insulation: typically made of insulation papers or laminates which insulate the winding from the grounded stator
- impregnation: typically made of resins which are inserted inside the slot after winding to replace the enclosed air
- additional parts like the slot wedge to ensure mechanical stability of the insulation

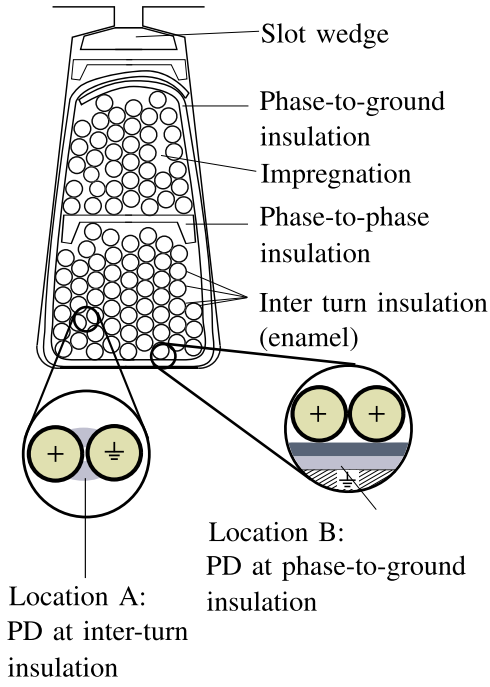

Fig. 1. Cross section of a slot.

Manuscript received July 23, 2020; revised November 13, 2020; accepted December 22, 2020. Date of publication December 29, 2020; date of current version August 20, 2021. Paper no. TEC-00749-2020. *(Corresponding author: Florian Pauli.)*

Florian Pauli, Niklas Driendl, and Kay Hameyer are with the Institute of Electrical Machines, RWTH Aachen University, 52062 Aachen, Germany (e-mail: florian.pauli@iem.rwth-aachen.de; niklas.driendl@iem.rwth-aachen.de; kay.hameyer@iem.rwth-aachen.de).

Moritz Kilper is with Mercedes-Benz AG, 70327 Stuttgart, Germany (e-mail: moritz.kilper@daimler.com).

Color versions of one or more figures in this article are available at https://doi.org/10.1109/TEC.2020.3048086.

Digital Object Identifier 10.1109/TEC.2020.3048086

In [6], the partial discharge inception voltage for all of these locations is studied for an exemplary insulation system using motorettes and an electric field FE-simulation. It is concluded that the lowest PD inception voltage occurs at the inter-turn insulation between two neighboring conductors. This justifies the large number of publications, which consider PD effects at the inter-turn insulation (location A in Fig. 1) [7]–[10]. A transient voltage leads to a high electric field strength between all components in the insulation system. The largest voltage between two components usually occurs between two phases, followed by the voltage between winding and stator iron. However, as the phase-to-phase and phase-to-ground insulation is made of insulation papers or laminates, which are thicker than the inter-turn insulation, it depends on the design of the insulation system, at which location PD will occur first.

To protect the insulation system from environmental stress and to improve its mechanical stability, impregnation material is inserted into the slot of the electrical machine. This material fills the air enclosures between neighboring enameled wires. As PD processes take place in those air enclosures, the threshold voltage for PD between neighboring conductors increases (location A in Fig. 1). The amount, position and size of air enclosures in the insulation system have a significant influence on the partial discharge inception voltage (PDIV) [11], [12]. The amount of impregnation material that is absorbed by the stator largely depends on the impregnation process [13]. PD can still occur at locations where air enclosures remain. Particularly between the phase-to-ground insulation and the stator, large air enclosures are common (location B in Fig. 1). The application of the impregnating material leads to an increased electric field strength between stator and phase-to-ground insulation. This increased field strength lowers the PDIV. The universal assumption that impregnating a stator automatically increases its PDIV is not applicable. To complement current research on PD effects, which mainly focuses on the inter turn insulation [7]–[10], the effect of impregnation material on PD processes between the winding and the grounded stator is studied in this work.

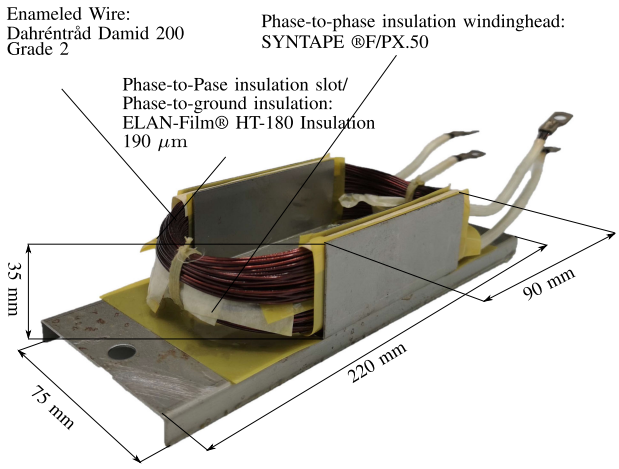

(a) Overall view of the motorette.

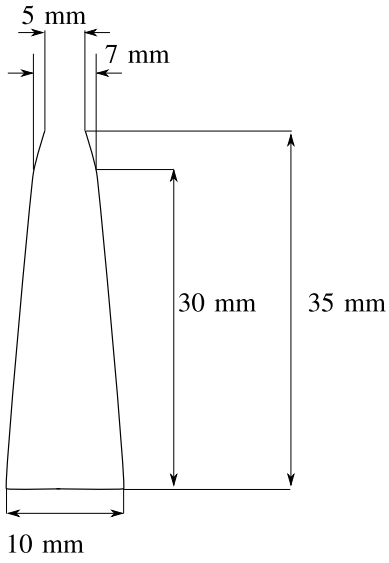

(b) Cross section of one slot.

Fig. 2. Motorette for initial studies. For the motorette which is displayed here, impregnation material is applied.

II. Initial Studies

First studies on the influence of impregnating material on the PDIV are performed by using motorettes. Two different types of motorettes are set up, one with and one without impregnation. Apart from that, the specimens are identical. In Fig. 2, the setup of the motorette is displayed along with its dimensions. The diameter of the applied winding wire is 1 mm. The winding consists of two layers where each winding has 7 turns and 10 conductors connected in parallel. In this paper, 20 motorettes of each type are studied. The PDIV is measured between the upper layer and the grounded metal sheet as well as the lower layer and the grounded metal sheet respectively. Contrary to the pulsed voltage which occurs at the terminals of inverter driven machines, in this paper a sinusoidal voltage with a frequency of 50 Hz is applied, which is suitable according to *IEC 60 034-18-41* [14]. Thus, the voltage drop between the winding and the grounded metal can be determined exactly and no transient effects must be considered. To measure PDIV and PDEV, a commercial type *Schleich MTC3* stator tester is used. In Fig. 3, boxplots of the results of the PDIV-measurement are displayed. The median PDIV is marked with the line in the center of the box. The box itself denotes the central two quartiles while the entire range of the measured voltage is marked with the whiskers. A large range of measurement values is generally caused by measurement uncertainties and variations in the quality of the specimens. Outliers are labeled with a '+'. They are caused by faulty measurements or defect motorettes. The measuring values of the PDIV refer to the amplitude of the testing voltage. For the configurations in Fig. 3(a), the achieved PDIV of the impregnated motorette is slightly lower than for the non-impregnated motorette, for the configuration in Fig. 3(b), the measured PDIVs for both motorette types are nearly identical. This opposes the general assumption that adding impregnating material leads to higher PDIVs. The measured partial discharge extinction voltages (PDEV) are displayed in Fig. 4. For the measurement

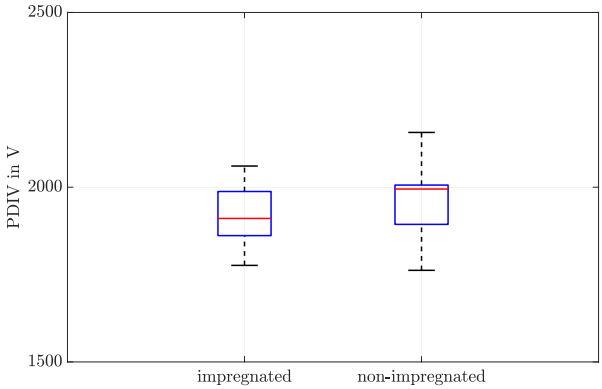

(a) PDIVs between the upper layer and grounded metal sheet.

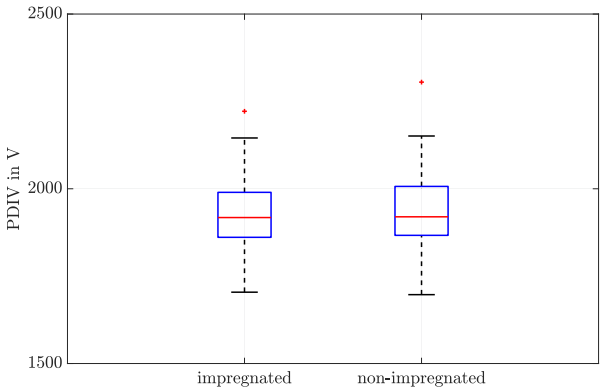

(b) PDIVs between the lower layer and grounded metal sheet.

Fig. 3. PDIVs for the phase-to-ground insulation in impregnated and non-impregnated motorettes.

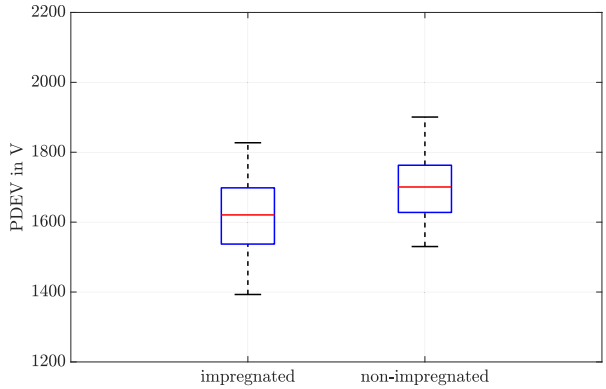

(a) PDEVs between the upper layer and grounded metal sheet.

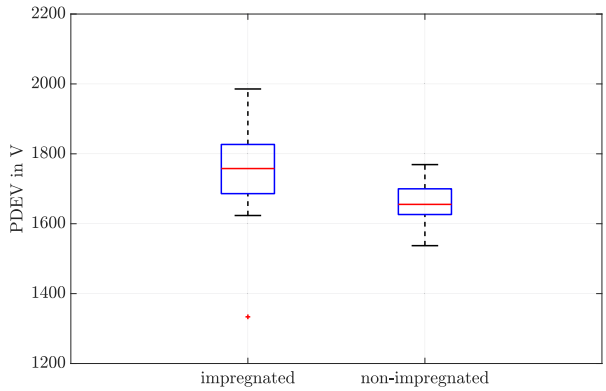

(b) PDEVs between the lower layer and grounded metal sheet.

Fig. 4. PDEVs for the phase-to-ground insulation in impregnated and non-impregnated motorettes.

between the upper layer and the grounded sheet construction, higher PDEVs are measured for the non-impregnated case while for the lower layer, the PDEVs for the impregnated case are higher. Thus, there is no significant difference between the PDEVs for impregnated and non-impregnated motorettes.

The winding of the motorettes, which are studied in the present paper, are preproduced by a flyer winding process where the tension of the wire is not controlled. The winding is then inserted into the slots manually. To fix the winding, a slot wedge made of NKN laminate and glas fiber strings in the winding head are used. The winding is impregnated by a simple dipping process and subsequently hardned in the oven in an upright position. As the process is conducted under normal pressure, air enclosures are likely to form inside the winding. Due to the fact the specimens are hardened in an upright position, it is probable that more impregnation material can be found in the lower layer of the motorette. This is a possible explaination for the difference of the measured PDIVs in Fig. 3(a) and Fig. 3(b). Apart from removing air enclosures from the winding, the application of impregnation changes the electric field distribution inside the winding, which can lead to an increased field strength in some locations of the insulation system. In the following, this effect is investigated, focusing on the junction between stator iron and the winding.

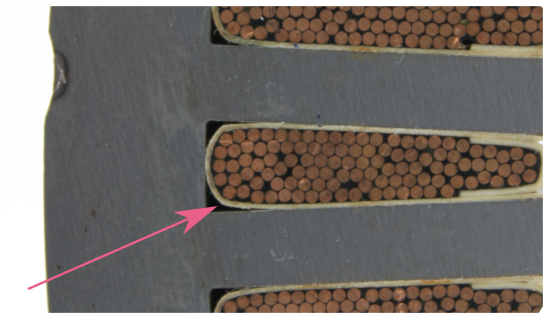

Fig. 5. Cross section of a slot.

III. Modeling of the Junction

A cross section of the slot of an exemplary electrical machine is displayed in Fig. 5. While the winding is filled with impregnating material there is a visible air gap between the phase-to-ground insulation and the stator with a maximum width of more than 1 mm. Even significantly smaller air gaps with a thickness in the range of 50 μm can lead to partial discharge. In [15], the thermal resistance of the junction between stator iron and winding is modeled. Air cavities due to material imperfections between stator iron and slot liner are considered by applying an artificial air gap which represents the average distance between

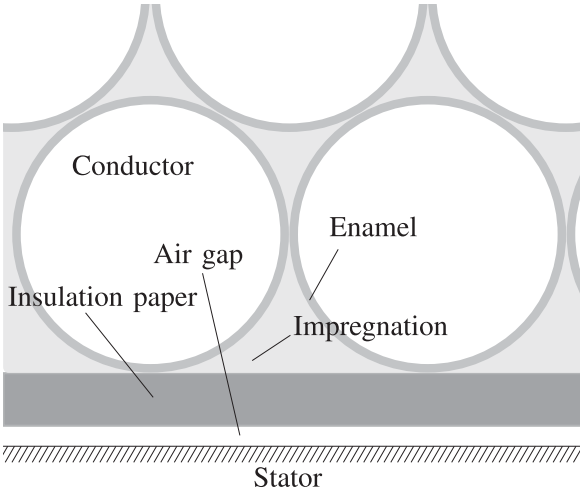

Fig. 6. Different regions in the insulation system of a traction drive.

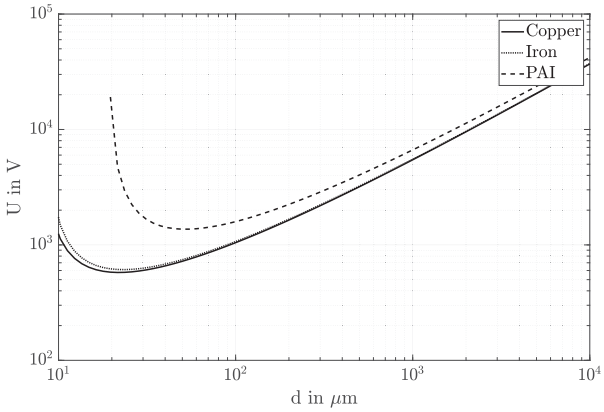

Fig. 7. *Paschen* curves for different cathode materials in air under normal pressure (1013 hPa).

phase-to-ground insulation and the stator iron that is produced by the cavities. The thickness of the artificial air gap in [15] is determined to be around 60 μm. As this thickness only represents an average width, it can be deduced that some cavities have larger diameters. At other locations there is a direct contact between the slot liner and the stator. At these locations, the width of the gap at the interface between winding system and stator is 0 μm. In the following, the influence of the presence of impregnation material on the side of the surface insulation, which is facing the interior of the winding, on partial discharge processes inside the airgap between slot liner and stator, is considered. For this purpose an electrostatic FE-simulation is performed and specimens, that allow to focus on the junction between stator iron and winding, are designed.

A. Fe-Model

To set up an FE-Model, which describes the aforementioned junction, four different regions of the insulation system are defined:

- The enamel coat on top of the conductors
- the insulation paper between the winding and the stator
- the impregnation material to fill the air enclosures between the conductors
- a remaining air gap between the insulation paper and the grounded stator

In Fig. 6, the different regions are displayed for a low voltage machine with a round wire winding. In order to simulate the electric field, the relative permittivities of the different regions are defined according to Table I.

In Table II, the dimensions of the components of the insulation system which is simulated in this paper are given. The thickness of the enamel surface corresponds to the median thickness of the insulation layer of an enameled wire of grade 2 according to the standard [16]. For the following calculation of the PDIV, the width of the air gap is varied from 0...1000 μm.

The electric field in the air gap is the highest perpendicular to the location where the round conductor touches the phase-to-ground insulation. Due to symmetry, the field that is caused by the neighboring wires does not influence the electric field in this location. For the non-impregnated insulation system, PD can also occur between the enameled wire and the insulation paper. With the model from [8] it can be shown that PD only occurs close to the location where the enameled wire and the insulation are in contact. At this location, the influence of the other wires on the electric field is low when compared to the field which is caused by the examined conductor. Therefore, only one wire is considered in the FE-Model. The resulting field density is displayed in Fig. 8. As the permittivity of the impregnation material is larger than the permittivity of air, the electric field close to the enameled wire is larger in the case where no resin is applied. The electric field in the air gap between phase-to-ground insulation is subsequently increased for the setup which considers the impregnating material as the applied voltage between conductor and stator is the same for both setups.

TABLE I
PERMITTIVITIES OF THE DIFFERENT REGIONS IN THE ELECTROSTATIC FE-MODEL

region	material	relative permittivity
enamel	polyamide-imide	4.2
insulation paper	polyaramide-polyimide laminate (NKN®)	3.1
impregnation	epoxy resin (Elan-protect®EP 201)	3.1
air gap	air	1.0

TABLE II
DIMENSIONING THE COMPONENTS FOR THE FE-SIMULATION

component	dimensions in μm
Ø conductor	1000
thickness insulation paper	300
thickness enamel	37.5
air gap	0.0...1000

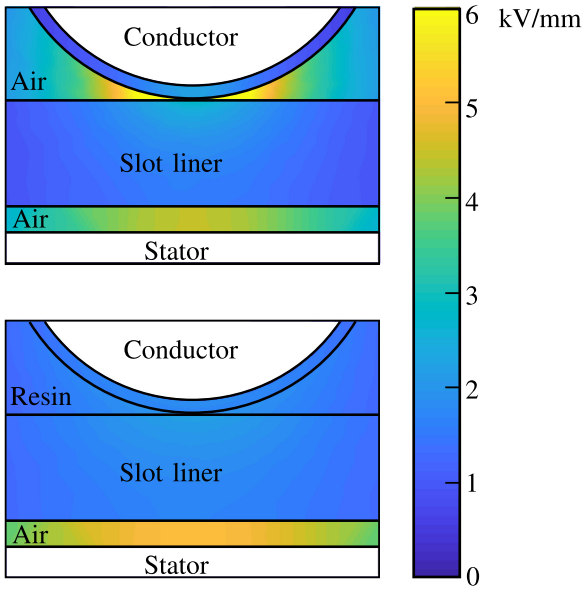

Fig. 8. Electric field solution for the considered setup and an applied voltage of 1 kV. Top: Field distribution without impregnation; bottom field distribution with impregnation applied.

TABLE III
PARAMETERS OF THE *TOWNSEND* EQUATION FOR AIR AND DIFFERENT CATHODE MATERIALS

parameter	material	value
A	air	$4.7\,\mathrm{Pa}^{-1}\,\mathrm{m}^{-1}$
B	air	$267\,\mathrm{V}\,\mathrm{Pa}^{-1}\,\mathrm{m}^{-1}$
γ	copper	0.025
	iron	0.020
	PAI	0.000 15

B. Discharge Process

According to the *Paschen* law, the minimum voltage U for a discharge process between two surfaces depends on air pressure p and the distance between the electrodes d, as well as on the properties of the surrounding gas and on the cathode material. The material properties are described by the parameters A, B and γ. The *Townsend* equation is used to calculate the *Paschen* curves for different cathode materials (cp. Fig. 7):

$$U = \frac{B \cdot p \cdot d}{\ln(A \cdot p \cdot d) - \ln\left(1 - \frac{1}{\gamma}\right)} \tag{1}$$

The parameters for the *Townsend* equation are chosen according to Table III [17]. The curves for the metallic materials copper and iron resemble each other, while the minimum voltage of the curve for the insulation material polyamide-imide (PAI) is significantly higher.

The PDIV is calculated by considering the electric field distribution and the *Paschen* curve analogous to [18]–[20]. The procedure to calculate the PDIV is illustrated in Fig. 9. If no impregnation is applied, PD can occur at two locations: between the enamel surface of the conductor and the phase-to-ground insulation (Fig. 10(a)) as well as between the phase-to-ground

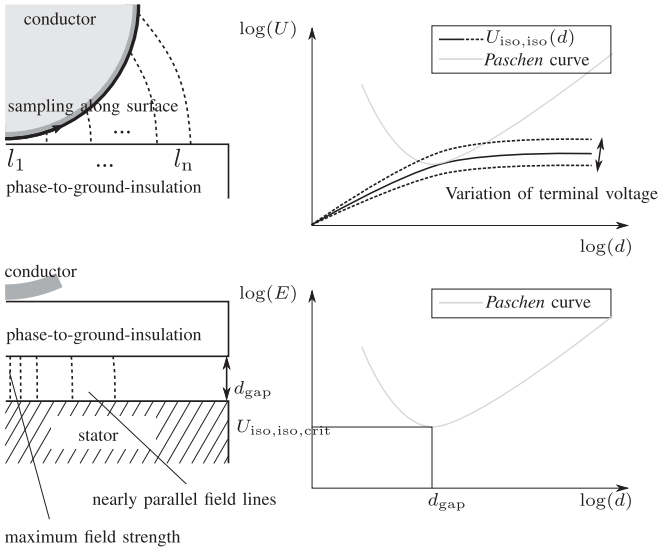

Fig. 9. PDIV calculation at different locations.

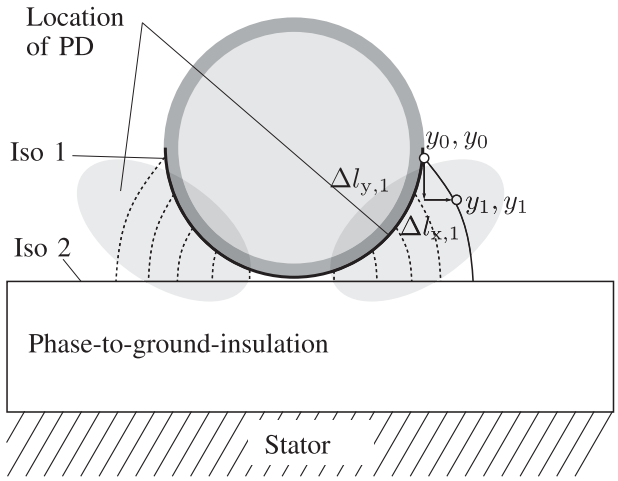

(a) PDIVs between the upper layer and grounded metal sheet.

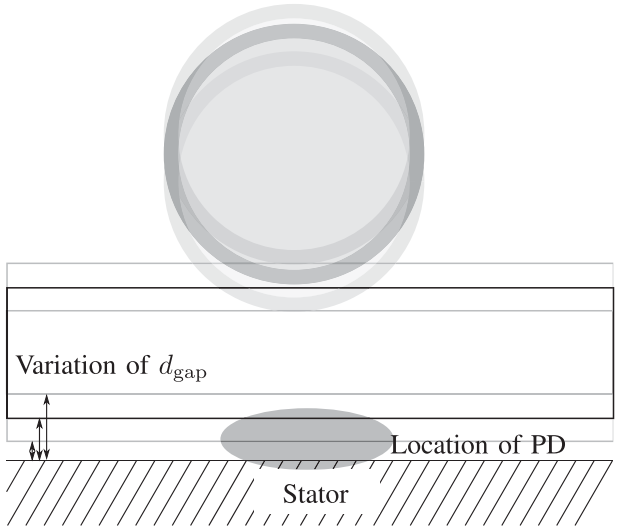

(b) PDIVs between the lower layer and grounded metal sheet.

Fig. 10. PDIVs for the phase-to-ground insulation in impregnated and non-impregnated motorettes.

insulation and the stator (Fig. 10(b)). To calculate the PDIV for the first case, the coated conductor surface is considered as the starting points of electric field lines, which end on the surface insulation. To caclulate the voltage drop between the two surfaces, the electric field E is integrated along a field line from one surface at the coordinates $(x, y)_0$ to the other one at the coordinates $(x, y)_\mathrm{k}$. This results into the voltage $U_{0,k}$ between the points $(x, y)_\mathrm{iso1}$ and $(x, y)_\mathrm{iso2}$ on different surfaces which are connected by the same field line:

$$U_{0,\mathrm{k}} = \int_{(x,y)_\mathrm{iso1}}^{(x,y)_\mathrm{iso2}} \vec{E}\mathrm{d}\vec{l} \tag{2}$$

For the discrete field solution this expression becomes:

$$U_{\mathrm{iso,iso}} = \sum_{i=0}^{k} E(x_i, y_i)_x \Delta l_{\mathrm{x},i} + E(x_i, y_i)\Delta l_{\mathrm{y},i}. \tag{3}$$

$E_\mathrm{x}(x, y)$ and $E_\mathrm{y}(x, y)$ are the x- and y-component of the electrical field at the coordinates (x,y). The numerical integration is initialized at a starting point on one of the insulation surfaces (x_0, y_0). A fixed step size Δl is defined. Depending on the direction of the electric field, $\Delta l_{\mathrm{x},i}$ and $\Delta l_{\mathrm{y},i}$ are calculated:

$$\begin{aligned} \Delta l_{\mathrm{x},i} &= \frac{E_\mathrm{x}, i}{\sqrt{E_{\mathrm{x},i}^2 + E_{\mathrm{y},i}^2}} \Delta l \\ \Delta l_{\mathrm{y},i} &= \frac{E_{\mathrm{y},i}}{\sqrt{E_{\mathrm{x},i}^2 + E_{\mathrm{y},i}^2}} \Delta l \end{aligned} \tag{4}$$

The coordinates are updated according to equation (5):

$$\begin{aligned} x_{i+1} &= x_i + \Delta l_{\mathrm{x},i} \\ y_{i+1} &= y_i + \Delta l_{\mathrm{y},i} \end{aligned} \tag{5}$$

The integration process is terminated, when the surface of the insulation $iso2$ is reached. The length of the field line $l_\mathrm{field\,line}$ is calculated according to equation (6).

$$l_\mathrm{field\,line} = \sum_{i=0}^{k-1} \sqrt{\Delta l_{x_i}^2 + \Delta l_{y_i}^2} \tag{6}$$

By sampling the field lines along the conductor surface, starting where the wire touches the phase-to-ground-insulation, and by evaluating the voltage drop each field line, the $U_\mathrm{iso,iso}$ in dependence of the distance between the surfaces d, which corresponds to the length of the field lines is obtained. A variation of the voltage between stator and conductor can be modeled by scaling the field strength. In the top right corner of Fig. 9, the voltage between the insulation surfaces is displayed for three exemplary terminal voltages. The solid line has exactly one point of contact with the *Paschen*-curve. Therefore, the minimum terminal voltage for a discharge process (cp. eq. (1)) is just reached. This voltage is considered the PDIV.

When modeling PD in the junction between stator iron and winding both, the stator iron and the insulation paper can be considered as the cathode, as an alternating voltage is applied. However, as the inception voltage for discharge processes is lower for metal surfaces (cp. Fig. 7), in the studied setup PD will first start from the metallic stator iron. Therefore, the stator core is considered as the cathode in the following. The field lines inside the air enclosure between stator and slot liner can be considered as parallel. From the setup of the specimens it can be concluded that the maximum field strength occurs at the point where the round conductor is the closest to the phase-to-ground-insulation. The *Paschen*-curve can be evaluated at this point to achieve the PDIV. For the impregnated specimens, PD can only occure between the stator and the slot liner.

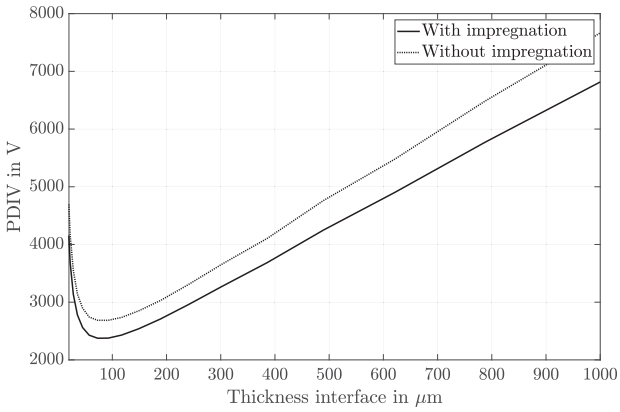

Fig. 11. Minimum voltage for a discharge process in the interface air gap.

For discharge processes between the enameled wire and the slot liner, a worst case scenario is achieved when the surface insulation material touches the stator (cp. Fig. 10(a)). Due to the characteristic of the *Paschen* curve, PD does not occur at locations where the insulation surfaces are the closest to each other. When assuming the material properties of PAI for both surfaces, the PDIV calculated for this case is 5860 V.

The PDIV between stator and slot liner is a function of the air gap width d_gap. In this paper, the air gap width is varied to obtain a worst-case estimate for the PDIV (cp. Fig. 10(b)). In Fig. 11, the calculated minimum voltage for a discharge process inside the air gap between stator iron and phase-to-ground insulation is displayed as a function of the interface width. The minimum PDIV for both, the impregnated and the non-impregnated setup appears at a width of 73 μm. The difference between the simulation results for both studied cases is more pronounced than the difference between the measuring results for the motorettes (Fig. 3). However, as the geometry of the motorettes is complex PD activity in the air enclosure between stator iron and phase-to-ground insulation cannot be considered isolated from other locations where PD might occur. In the following, a specimen with a more simple geometry is set up in such a way that the location of PD is determined by the test piece's design.

C. Proposed Specimen Design

The proposed specimens consist of a bare copper flat wire which is wrapped into a polyaramid-polyimide laminate (NKN). An enameled wire is manually wound around the wrapped, flat copper wire. To apply a well defined force, a weight of 1 kg is attached to the enameled wire. The production process is displayed in Fig. 12. The bare copper rod in this setup simulates

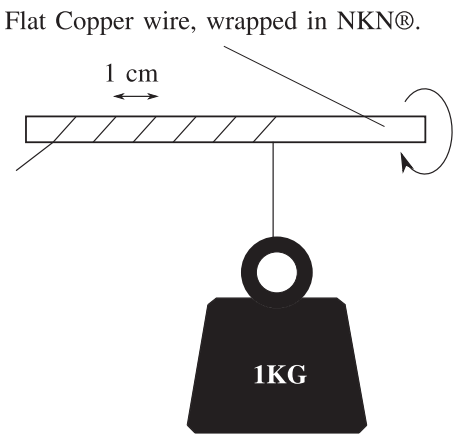

Fig. 12. Production process of the proposed specimen.

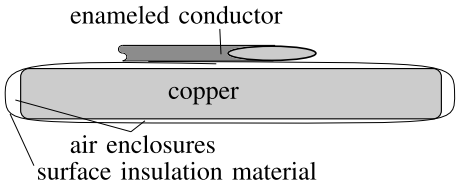

(a) schemetics of the cross section of the proposed specimen.

(b) Photo of the proposed specimen.

Fig. 13. Proposed specimen.

the stator core. Copper wire instead of iron is chosen due to the easier handling and availability. As shown in Fig. 7, the discharge characteristics of both materials are almost identical. A flat conductor is chosen in order to create an air gap with a non-uniform size between the copper rod and the surface insulation material (cp. Fig. 13(a)). As the weakest point in the specimen defines the PDIV, it can be assumed that the worst-case air gap thickness is reached at least for one location of the specimen. To ensure that the impregnation material is not entering into the air enclosure between the NKN and the bare copper wire, it is directly applied on the preheated specimen using a syringe. The preheating causes the impregnation material to gel as soon as it touches the specimen. An impregnated specimen is displayed in Fig. 13(b).

By disassembling two impregnated specimens, it is verified that no impregnation material can be found between the bare copper and the surface insulation. The material properties of the specimens are listed in Table IV.

IV. PDIV Measurement and Discussion

The PDIV between the bare and the enameled copper wires is measured. Again, a commercial *Schleich MTC3* testing device

TABLE IV
Components of the Proposed Specimen

component	simulated machine component	properties
bare copper wire	stator	flat wire bare copper 1 mm × 4 mm
enamelled wire	winding wire	enamel material: PAI Ø 1 mm grade 2
insulation paper	phase-to-ground insulation	NKN® thickness: 300 µm
impregnation	impregnation	epoxy resin Elan-protect® EP 201

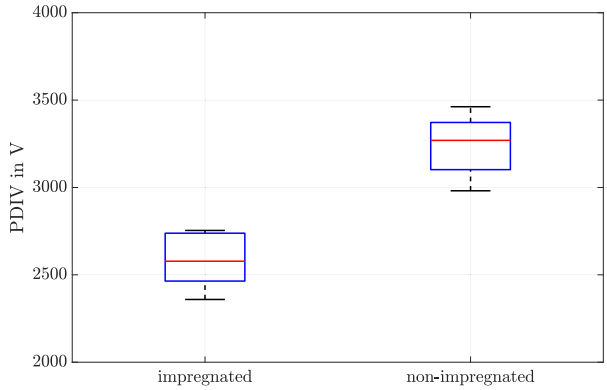

(a) Measuring results ot the PDIV-measurement.

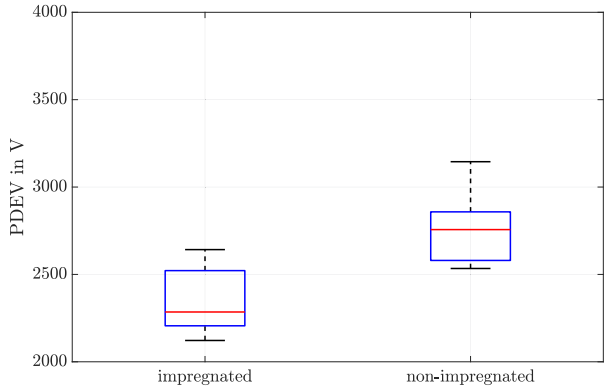

(b) Measuring results ot the PDEV-measurement.

Fig. 14. PDIV and PDEV of impregnated and non-impregnated specimens.

is utilized. In the same way as for the motorettes in the initial studies, a sinusoidal testing voltage with a frequency of 50 Hz is applied. The temperature is kept constant at 22° (± 1K) using air conditioning. The humidity is monitored during the PDIV measurement. It remains in a range between 55% and 60%. Ten specimens of each type (impregnated and non-impregnated) are considered. The measured PDIVs are displayed in Fig. 14(a).

Except from one outlier, all measured PDIVs of the non impregnated specimens are higher than those of the impregnated specimens. When impregnating the specimens, the average measured PDIV drops from 3269 V to 2578 V which is a decrease by 21.1%. The calculated PDIVs are slightly lower: 2687V and 2375V respectively. This corresponds to a decrease by 11.6%. The measured PDEVs drop from an average of 2756 V to 2285 V (cp. Fig. 14(b)).

The deviation between the measured and calculated PDIVs can be explained by the application of the *Paschen*-curve and by manufacturing deviations of the insulation materials:

- The *Paschen* curve is only defined for homogeneous electrical fields while the field in the air gap of the presented set up is not homogeneous.
- Different parametrizations of the *Paschen* curve in literature (e.g. [17], [21], [22]) provide inconsistent simulation results for the PDIV.
- Deviation of air pressure, temperature and humidity influence the measuring results.
- The thickness of the surface insulation material and of the enameled wire can deviate from the data which is supplied by the manufacturer.
- Imperfections of the cathode surface change the PDIV.

Deviations between the behavior of the motorette for the initial tests and developed specimens can be explained by the advanced complexity and the different impregnation material of the motorettes with unknown dielectric properties. In general, the decrease of the PDIV is less pronounced, if the permittivity of the impregnation material is low. If the impregnation is applied such that the void between stator iron and surface insulation material is entirely filled, PD at the interface between stator and winding will be prevented, leading to higher PDIVs even compared to the case where no impregnation is applied. To achieve this, a suitable impregnation process must be applied. The capability of different impregnation processes to achieve a filled void between stator lamination and the surface insulation material is discussed in the following. Trickling is a common impregnation process where a fine jet of impregnation resin is poured on the winding head. Due to the cappilar effect, the material is transported into the slots [13]. Without modification such a process is not capable to apply impregnation material between the lamination and the surface insulation. During a dipping process, the stator is at least partly inserted into the resin. In this case, the impregnation can enter the void, especially when vacuum impregnation is applied. To improve resin absorption, an electric current can be applied between the terminals of the stator. This will cause the winding to heat up and the impregnation material close to the winding to gel [13]. Regarding the void betweeen stator lamination and surface insulation however, the surface insulation also acts as an thermal insulation. To achieve a gelling in the void, longer heating times may be applied. However, this might lead to impregnation absorption at undesired locations. The motorettes, which are applied in this paper, are preheated inside an oven and thereupon dipped into the impregnation resin. The preheating causes an increased viscosity of the resin and therefore prevents the enamel from filling all airgaps.

V. Conclusion

In this paper, a methodology to model partial discharge in the junction between the winding and the stator iron is presented. In motorettes PD can occur at various locations. Therefore, a type of specimen is proposed which allows to consider PD processes between the stator and the phase-to-ground insulation isolated from other PD activities. Additionally, a simulation model which is based on the electric field strength in the setup is presented. Between winding and stator, PD can occur at two locations if no impregnation material is applied: in air enclosures between stator lamination and the phase-to-ground insulation as well as between the phase-to-ground insulation and the enameled wires of the winding. For the examined setup, it can be shown that PD fist starts in the air encapsulations between stator and insulation paper. The influence of impregnating material on the PDIV at this location is examined. Both, simulation model and measurement show that the PDIV at this location is decreased, when adding impregnation material, which opposes the general assuption that impregnating a winding always leads to an increased PDIV. This finding emphasises the importance of prototype based tests (e.g. motorettes) when designing insulation systems even though generalized design rules are available. The effect of a decreased PDIV is caused by an increase of the electric field inside the air enclosures which takes place when impregnation material is added to the winding. Applying an impregnation process, which only leaves air enclosures that are significantly smaller than the distance at the *Paschen* minimum, would prevent this effect.

References

[1] S. Hazra *et al.*, "High switching performance of 1700-V, 50-A SiC power MOSFET over Si IGBT/BiMOSFET for advanced power conversion applications," *IEEE Trans. Power Electron.*, vol. 31, no. 7, pp. 4742–4754, Jul. 2016.

[2] M. Melfi, J. Sung, S. Bell, and G. Skibinski, "Effect of surge voltage risetime on the insulation of low voltage machines fed by pwm converters," in *Proc. IAS '97. Conf. Record 1997 IEEE Ind. Appl. Conf. 32nd IAS Annu. Meeting*, Oct 1997, vol. 1, pp. 239–246.

[3] O. Magdun, S. Blatt, and A. Binder, "Calculation of stator winding parameters to predict the voltage distributions in inverter fed ac machines," in *Proc. 9th IEEE Int. Symp. Diagn. Electric Mach., Power Electron. Drives*, Aug. 2013, pp. 447–453.

[4] S. Mahdavi and K. Hameyer, "High frequency equivalent circuit model of the stator winding in electrical machines," in *Proc. 20th Int. Conf. Elect. Mach.*, Sep. 2012, pp. 1706–1711.

[5] R. Maier and M. Bakran, "SiC effect on surge voltage distribution in large electrical machines," in *Proc. PCIM Europe 2018 - Int. Exhib. Conf. Power Electron., Intell. Motion, Renewable Energy and Energy Manage.*, Jun. 2018, pp. 853–859.

[6] V. Madonna *et al.*, "Reliability vs. performances of electrical machines: Partial discharges issue," in *Proc. IEEE Workshop Elect. Mach. Des., Control Diagnosis*, Apr. 2019, vol. 1, pp. 77–82.

[7] L. Lusuardi *et al.*, "Design criteria for inverter-fed type 1 motors," in *Proc. IEEE Int. Conf. Dielectrics*, vol. 2, Jul. 2016, pp. 605–608.

[8] N. Driendl, F. Pauli, and K. Hameyer, "Modeling of partial discharge processes in winding insulation of low-voltage electrical machines supplied by high $\mathrm{d}u/\mathrm{d}t$ inverters," in *Proc. IECON 2019-45th Annu. Conf. IEEE Ind. Electron. Soc.*, vol. 1, Oct. 2019, pp. 7102–7107.

[9] T. Rokunohe, T. Kato, H. Kojima, N. Hayakawa, and H. Okubo, "Calculation model for predicting partial-discharge inception voltage in a non-uniform air gap while considering the effect of humidity," *IEEE Trans. Dielectr. Electr. Insul.*, vol. 24, no. 2, pp. 1123–1130, Apr. 2017.

[10] D. Fabiani, G. C. Montanari, A. Cavallini, and G. Mazzanti, "Relation between space charge accumulation and partial discharge activity in enameled wires under pwm-like voltage waveforms," *IEEE Trans. Dielectr. Electr. Insul.*, vol. 11, no. 3, pp. 393–405, Jun. 2004.

[11] S. Hirabayashi, Y. Shibuya, T. Hasegawa, and Y. Inuishi, "Estimation of the size of voids in coil insulation of rotating machine," *IEEE Trans. Elect. Insul.*, vol. EI- 9, no. 4, pp. 129–136, Dec. 1974.
[12] M. U. Zuberi, A. Masood, E. Husain, and A. Anwar, "Estimation of partial discharge inception voltages due to voids in solid sheet insulation," in *Proc. IEEE Elect. Insul. Conf.*, Jun. 2013, pp. 124–128.
[13] J. Richnow, P. Stenzel, A. Renner, D. Gerling, and C. Endisch, "Influence of different impregnation methods and resins on thermal behavior and lifetime of electrical stators," in *Proc. 4th Int. Electric Drives Prod. Conf.*, Sep. 2014, pp. 1–7.
[14] IEC 60034-18-41, "Rotating electrical machines - part 18-41: Partial discharge free electrical insulation systems (type i) used in rotating electrical machines fed from voltage converters - Qualification and quality control tests," *IEC*, 2014.
[15] R. Wrobel, S. J. Williamson, J. D. Booker, and P. H. Mellor, "Characterizing the in situ thermal behavior of selected electrical machine insulation and impregnation materials," *IEEE Trans. Ind Appl.*, vol. 52, no. 6, pp. 4678–4687, Nov./Dec. 2016.
[16] International electrotechnical comission, "pecifications for Particular Types of Winding Wires - Part 0-1: General Requirements - Enamelled Round Copper Wire," Standard IEC 60317-0-1, 10 2013.
[17] A. E. D. Heylen, "Sparking formulae for very high-voltage paschen characteristics of gases," *IEEE Elect. Insul. Mag.*, vol. 22, no. 3, pp. 25–35, May/Jun. 2006.
[18] V. Madonna, P. Giangrande, W. Zhao, H. Zhang, C. Gerada, and M. Galea, "On the design of partial discharge-free low voltage electrical machines," in *Proc. IEEE Int. Electric Mach. Drives Conf.*, May 2019, pp. 1837–1842.
[19] C. Philippe, M. David, and L. Yvan, "Tool to design the primary electrical insulation system of low voltage rotating machines fed by inverters," in *Proc. IEEE Elect. Insul. Conf.*, Jun. 2018, pp. 8–13.
[20] F. Pauli, N. Driendl, and K. Hameyer, "Study on temperature dependence of partial discharge in low voltage traction drives," in *Proc. IEEE Workshop Elect. Mach. Des., Control Diagnosis*, vol. 1, Apr. 2019, pp. 209–214.
[21] A. N. Prasad, "Measurement of ionization and attachment coefficients in dry air in uniform fields and the mechanism of breakdown," *Proc. Phys. Soc.*, vol. 74, no. 1, pp. 34–41, Jul. 1960.
[22] A. N. Prasad and J. D. Craggs, "Measurement of ionization and attachment coefficients in humid air in uniform fields and the mechanism of breakdown," *Proc. Phys. Soc.*, vol. 76, no. 2, pp. 223–232, Aug. 1960.

Florian Pauli received the M.Sc. degree in electrical engineering from the RWTH Aachen University, Germany, in April 2017. He has been working as a Research Associate with the Institute of Electrical Machines since May 2017. His research interests include iron loss computations, thermal behavior, overload capability, lifetime models, and the characterization of insulation systems of electrical machines.

Moritz Kilper received the M.Sc. degree in automotive and engine engineering from the University of Stuttgart, Germany, in December 2017. He is currently employed by Mercedes-Benz AG with the Advanced Engineering of Electrical Motor Systems as a Ph.D. Student, supervised by Prof. Hameyer with the Institute of Electrical Machines, RWTH Aachen University. His research interests include materials for electrical machines with a focus on insulation systems of electrical machines.

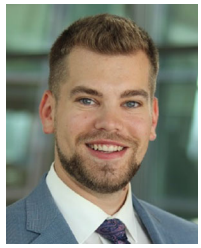

Niklas Driendl received the M.Sc. degree in electrical engineering from the RWTH Aachen University, Germany, in October 2018. In January 2019, he started working as a Research Associate with the Institute of Electrical Machines, RWTH Aachen University, Germany. His research interests include the characterization of insulation systems and modeling of partial discharge processes.

Kay Hameyer (Senior Member, IEEE) received the M.Sc. degree in electrical engineering from the University of Hannover and the Ph.D. degree from the Berlin University of Technology, Germany. After his university studies, he worked with the Robert Bosch GmbH in Stuttgart, Germany as a Design Engineer for permanent magnet servo motors and vehicle board net components. From 1996 to 2004, he was a Full Professor of Numerical Field Computations and Electrical Machines with the KU Leuven in Belgium. Since 2004, he is a Full Professor and Director of the Institute of Electrical Machines (IEM) with the RWTH Aachen University, Germany. In 2006, he was the Vice Dean of the Faculty and from 2007 to 2009, he was the Dean of the Faculty of Electrical Engineering and Information Technology of RWTH Aachen University. He has authored more than 250 journal publications, more than 700 international conference publications and author of four books. His research interests include numerical field computation and optimization, the design and controls of electrical machines, in particular permanent magnet excited machines and induction machines. For several years, his work is concerned with magnetically excited audible noise in electrical machines, the life time estimation of insulating systems and the characterization of ferro-magnetic materials. He is also a member of VDE and a fellow of the IET.